Finite Control Set Model Predictive Control with Feedback Correction for Power Converters

Kun Shen, Jianghua Feng, and Jing Zhang, *Member, CES*

***Abstract*—As an open-loop model predictive control algorithm, finite control set model predictive control (FCS-MPC) scheme in power converter system is based on assumption that responses of optimal control implemented on prediction model agree well with actual system. The influence of model parameter mismatches and environment disturbance on control performance of scheme is neglected. Then, based on feedback correction strategy in traditional model predictive control algorithm, we derive a finite control set model predictive control with feedback correction scheme (FCS-MPCFC) that allows us to adjust prediction model output at current instant by model prediction error at previous instant, and the closed-loop correction of prediction model output is achieved. Simulations comparison analyses on a two-level three-phase inverter with multi-type model parameter mismatches controlled by traditional and improved FCS-MPC scheme are presented. Experiments are carried out on DSP controller platform.**

***Index Terms*—FCS-MPC, feedback correction, parameter mismatches, power converter, robustness.**

I. Introduction

MODEL predictive control (MPC) is a kind of optimal control scheme with characters of adaptability and robustness. This scheme generally consists of prediction model, cost function and feedback correction strategy. The feedback correction strategy in MPC is an important guarantee of robustness and parametric self-adaptability, this simple strategy is useful in industrial application [1]. During the last decade, finite control set model predictive control (FCS-MPC) scheme for power converter system has received considerable attention where it contributes with several advantages such as intuitive modeling, straightforward handing of constrains and fast dynamic performance [2–16].In FCS-MPC scheme, based on the fact that switch combinations of one converter are finite, system output created by each switch combination can be calculated by prediction model respectively, and the optimal control sequence is a switch combination which minimizes the designed cost function [3].The computational problem, stability, low switcher loss and closed-loop performance of FCS-MPC scheme are hot topics in literatures [2–9]. The delay compensation method for FCS-MPC is presented in [4]. In [5], an intermediate sampling method is used to improve steady-state performance of FCS-MPC. As an optimal control scheme for power electronics system, in FCS-MPC, reducing switching frequency and improving waveform quality are challenges which should be faced in practice application. In [6], the switching frequency is reduced by designing cost function in transient operation and steady-state operation respectively, and in steady-state operation the minimum switching frequency is realized by a state graph. The design of weighting factors in cost function is another important problem for FCS-MPC scheme, but in [7] the cost function is designed without weighting factors. As an MPC scheme, long prediction horizons are required to ensure stability and control performance. Some ingenious methods are proposed for multistep FCS-MPC, such as heuristic search strategy [8], sphere decoding algorithm [9].

It is noticed that literatures related to FCS-MPC scheme mainly focus on constructing prediction model, designing cost function and solving computational burden to achieve better control performance for different application, but influences caused by model parameter mismatches and external disturbance are ignored. So robustness and disturbance rejection ability of FCSMPC scheme receive more attention recently [10–15].In [10], based on feedback correction strategy in traditional MPC algorithm, a modeling error compensation method is designed for FCS-MPC to compensate prediction error of a three-phase inverter prediction model. Furthermore, the influence of model parametric uncertainties on the prediction error of FCS-MPC for current control in a three-phase inverter is analyzed in [11]. In order to improve the system disturbance rejection ability and robustness of predictive torque control for induction motor systems, a disturbance observer is developed in [12] to overcome load torque disturbance, parameter uncertainties, and time delays. To achieve steady-state accuracy, [13] extends system model of DFIG with LC filter and introduces integral error feedback in MPC structure.

As the further work of [10], this paper pays attention to constructing feedback correction strategy for multistep FCS-MPC scheme, and a finite control set model predictive

Manuscript was submitted for review on 29, April, 2018.
This work was supported in part by the Natural Science Foundation of Hunan Province, China under Grant 2015JJ6070
Kun Shen is with the College of Electrical and Information Engineering, Hunan University, Changsha 410082, China(e-mail: shenkun@hnu.edu.cn)
Jianghua Feng is with the Technology Center of Zhuzhou CRRC Times Electric Co., Ltd., Zhuzhou 412001, China (e-mail: fengjianghua@teg.com).
Jing Zhang is with the College of Electrical and Information Engineering, Hunan University, Changsha 410082, China(e-mail: zhangjing@ hnu.edu.cn)
Digital Object Identifier 10.30941/CESTEMS.2018.00039

control with feedback correction (FCS-MPCFC) scheme for power converters system is proposed. The principle of FCS-MPC scheme and influence from model parameter mismatches and environment disturbance are discussed in Section II, while Section III shows the improved FCS-MPC scheme for power converters system. Simulation comparisons and experimental results are described in Section IV and V respectively. Conclusions are provided in Section VI.

II. Principle of FCS-MPC

A. Principle

FCS-MPC scheme is a kind of model predictive control algorithm for power converter system. This scheme is organized by the feature that switch combinations of one converter system are finite, which means finite control set, so control sequence during any control interval will be one of these switch combinations. The prediction model of converter system is built by the relationship between switch combination and controlled variables, and a cost function is designed for some control goals. In one control period, for each switch combination in the finite set, prediction model is used to calculate prediction values of controlled variables at next control instant. Then cost function estimates each prediction value, and the switch combination which minimizes cost function is selected as the optimal control sequence of system in next control interval. So large computational burden is a shortage of FCS-MPC scheme. But with rapid development of DSP and FPGA, the advantages like flexibly modeling, easily realizing control goals and constrains have attracted more attention.

The design process of FCS-MPC scheme for power converter system is described as follow. Firstly, prediction model $f_p\{x,S\}$ is built by controlled variable x and switch combination S. At sampling instant t_k, prediction value of controlled variable at instant t_{k+1}, $x_p(t_{k+1})$ is calculated by prediction model, i.e., $x_p(t_{k+1})=f_p\{x(t_k),S(t_k)\}$,where $x(t_k)$ is measured value and $S(t_k)$ is control sequence of instant t_k. Then prediction values of controlled variable at instant t_{k+2}, $x_{pi}(t_{k+2})$ are calculated, $x_{pi}(t_{k+2})=f_p\{x_p(t_{k+1}),S_i\}$,$i$=1,…,$n$, where n is the number of switch combinations in converter and S_i is one of switch combinations. The cost function $f_g\{x^*,x_{pi},S_i\}$ is built by desired control goals and constrains, such as tracking reference curve, reducing switching losses and other system constrains. And x^* is reference of controlled variable, which is considered smooth relative to control period. Lastly, switch combination S_i which minimizes cost function f_g is selected as the optimal control sequence of instant t_{k+1}. The structure diagram of FCS-MPC scheme for power converters is showed in Fig.1(a). The prediction model f_p and cost function f_g are included in FCS-MPC scheme. And during one control interval, f_p is computed n+1 times, while f_g is computed n times.

According to the principle of FCS-MPC scheme described above, it is assumed that control goal of converter system is controlled variable x tracking reference x^*. The operation process of FCS-MPC is presented in Fig.1(b). Green line is reference value curve x^*, red line is measured value curve of controlled variable which is the response of optimal control sequence $S(t_{k-1})$, black lines are prediction value curves, and black dashed line is selected prediction value curve which minimizes cost function. At instant t_k, prediction value $x_p(t_{k+1})$ is calculated firstly, and then prediction value of instant t_{k+2}, $x_{pi}(t_{k+2})$, i=1,…,n, are available. The switch combination S_i , $i \in \{1,…,n\}$,with least error between prediction value and reference value at instant t_{k+2} is selected as the optimal control sequence at instant t_{k+1}.

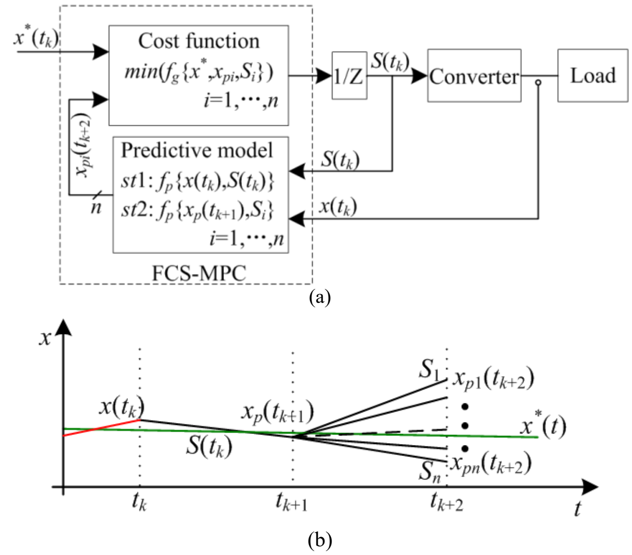

Fig. 1. Principle of FCS-MPC. (a) Structure. (b) Operation process.

B. Influence of Model Mismatches

In process of constructing FCS-MPC scheme, there is an assumption that prediction value calculated by prediction model agrees with measured value, so influence from model parameter mismatches and environment disturbance on control performance is neglected. The prediction model lacks closed-loop correction from actual system, and model prediction error will exist or enhance during whole control process.

The operation process of traditional FCS-MPC scheme with model mismatches considered is described in Fig.2. At instant t_k, since the existence of model mismatches, prediction value $x_p(t_k)$ do not equal to measured value $x(t_k)$, so the optimal control sequence $S(t_k)$ operates on system in the state of $x(t_k)$ and optimization calculation of $S(t_{k+1})$ works as well. Then black dashed line is derived from state $x_p(t_{k+1})$. At instant t_{k+1}, measured value $x(t_{k+1})$ is available, the prediction calculation of $x_p(t_{k+2})$ is carried out, and black dashed line will be translated parallel from point $x_p(t_{k+1})$ to $x(t_{k+1})$, then red dashed line appears in Fig.2.The parallel translation of response curve is

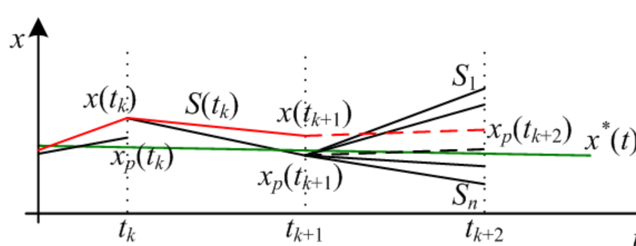

Fig. 2. FCS-MPC with model mismatches considered.

reasonable as that switch combination is held constant during each control interval, so converter system can be operated like linear system. In Fig.2, it is clearly indicated that prediction value $x_p(t_{k+2})$ is not in the expected state designed at instant t_k and the point is far from reference curve, which means that with existence of model mismatches, the selected control sequence may not be optimal when it works.

III. FCS-MPCFC

A. FCS-MPCFC Scheme

According to analysis in Section II part *B*, an open-loop structure exists in FCS-MPC, and the control performance of FCS-MPC has been impacted. While in classical MPC, feedback correction strategy is used to weaken influence from model parameter mismatches and external disturbance. Then based on feedback correction strategy, we propose a finite control set model predictive control with feedback correction (FCS-MPCFC) scheme for power converters. In this scheme, model prediction error of next control instant is adjusted by which of current control instant, so the feedback correction structure is achieved. The FCS-MPCFC scheme for power converter is showed as follow

*Step*1: at instant t_k, $x(t_k)$ is measured in system sampling process and $S(t_k)$ is optimal control sequence provided by scheme in last control interval and will operate on system in this control interval. $x_p(t_{k+1})$ is computed by prediction model f_p, i.e., $x_p(t_{k+1})=f_p\{x(t_k),S(t_k)\}$.

*Step*2: the first step closed-loop correction is achieved by

$$x_{cp}(t_{k+1}) = x_p(t_{k+1}) + \lambda_c\,[x_{cp}(t_k) - x(t_k)]. \tag{1}$$

Where $x_{cp}(t_k)$ is prediction value calculated in last control interval and has been adjusted, $x_{cp}(t_{k+1})$ is prediction value of t_{k+1} and will been adjusted at instant t_k. The correction factor λ_c is defined as

$$\lambda_c = \begin{cases} -0.5 & |x_{cp}(t_k) - x(t_k)| > \varepsilon \\ 0 & |x_{cp}(t_k) - x(t_k)| \le \varepsilon \end{cases}. \tag{2}$$

Where ε is error limen and is tuned by experiments. The control performance impacted by ε is analyzed in Section IV part *D*.

*Step*3: prediction values $x_{pi}(t_{k+2})$ are calculated by

$$x_{pi}(t_{k+2}) = f_p\left\{x_{cp}(t_{k+1}), S_i(t_{k+1})\right\} + \lambda_{c1}\,[x_{cp}(t_k) - x(t_k)]. \tag{3}$$

Where i=1,…,n, n is the number of switch combinations in converter and $S_i(t_{k+1})$is one of switch combinations, λ_{c1} is defined as

$$\lambda_{c1} = \begin{cases} -0.25 & \lambda_c \ne 0 \\ 0 & \lambda_c = 0 \end{cases}. \tag{4}$$

*Step*4: cost function $f_g\{x^*, x_{pi}(t_{k+2}),S_i(t_{k+1})\}$, i=1,…,n are calculated. The switch combination S_{imin}, $imin \in \{1,\dots,n\}$, which minimizes cost function is selected as optimal control sequence at instant t_{k+1} and will work during next control interval.

The value of correction factor λ_c and λ_{c1} is designed by experience and experiments. λ_c in (1) is used to adjust the output of prediction model at k+1 instant, and λ_{c1} in (3) is used to adjust the output of prediction model at k+2 instant. But at k instant, modeling errors of k+1 instant and k+2 instant are unobtainable, only the modeling error of k instant is available, so we use the modeling error of k instant to adjust the output of prediction model at k+1 and k+2 instant. This approximate calculation is based on the fact that the control period is much smaller than system period, and in a few control periods the system can be treated as linear system. In this paper, a conservative strategy is used to design parameters, and λ_c=1/2, λ_{c1}=1/4, which means that the modeling error of k+1instant is a half of which at k instant, and the modeling error of k+2 instant is a quarter of which at k instant. This approximate processing method is already applied in traditional MPC algorithm [1].

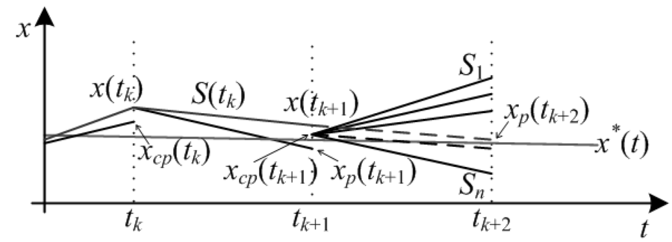

Fig. 3. Operation process of FCS-MPCFC.

The principle of FCS-MPCFC scheme is described in Fig.3, and the control goal in Fig.3 is tracking reference $x^*(t)$. At instant t_k, it is an assumption that error between measured value $x(t_k)$ and adjusted prediction value $x_{cp}(t_k)$ exists, so optimal control sequence $S(t_k)$ works on power converter system in state $x(t_k)$, and prediction value of instant t_{k+1}, $x_p(t_{k+1})$ is calculated, then closed-loop correction is achieved by (1). The prediction values of instant t_{k+2} are computed by (3), and the optimal response curve is chosen as black dashed line showed in Fig.3. Then at instant t_{k+1}, the optimal response curve will be translated parallel to state $x(t_{k+1})$, and prediction value $x_p(t_{k+2})$ is available. Since state variables like voltage and current in converter system are continuous and the mutation is disallowed, the designed correction process is reasonable. Compared with Fig.2, in Fig.3, the adjusted prediction value $x_{cp}(t_{k+1})$ is closer to measured value, and optimal control performance is held based on control sequence calculated by $x_{cp}(t_{k+1})$.

B. FCS-MPCFC for Three-phase Inverter

In this part, a two level three-phase voltage source inverter (2L-VSI) showed in Fig.4 is taken as an example to test the proposed FCS-MPCFC scheme. The switching function defined in Fig.4 is $S_j = S_{jp} = \overline{S_{jn}}$, j=a, b, c, and $S_j \in \{0,1\}$.Then switch combination is organized as S=[S_a, S_b, S_c]$^{\mathrm{T}}$, and there are 8 switch combinations in 2L-VSI, which are named S_i, i=0,…,7.

The FCS-MPCFC derives from FCS-MPC, so FCS-MPC scheme of 2L-VSI should be provided firstly. FCS-MPC scheme of 2L-VSI is described as follow [16].

Prediction model of 2L-VSI is

$$v_{op}(k+1) = \begin{bmatrix} 0 & 1 \end{bmatrix} \cdot \left[\boldsymbol{A}_q x(k) + \boldsymbol{B}_q v_s(k) + \boldsymbol{B}_{dq} i_o(k) \right]. \tag{5}$$

Where $x(k) = \begin{bmatrix} i_s(k) \\ v_o(k) \end{bmatrix}$, $\boldsymbol{A}_q = e^{AT_s}$ $\boldsymbol{B}_q = \int_0^{T_s} e^{A\tau}\boldsymbol{B}d\tau$

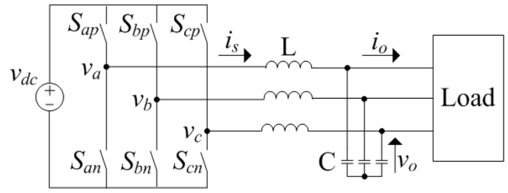

Fig. 4. 2L-VSI.

$\boldsymbol{B}_{dq}=\int_0^{T_s} e^{A\tau}\boldsymbol{B}_d d\tau$ and system matrix $\boldsymbol{A}=\begin{bmatrix}-\mathrm{r}/\mathrm{L} & -1/\mathrm{L}\\ 1/\mathrm{C} & 0\end{bmatrix}$, input matrix $\boldsymbol{B}=\begin{bmatrix}1/\mathrm{L} & 0\end{bmatrix}^{\mathrm{T}}$, interference input matrix $\boldsymbol{B}_d=\begin{bmatrix}0 & -1/\mathrm{C}\end{bmatrix}^{\mathrm{T}}$, T_s is sampling time, L is filter inductor, C is filter capacitor, and r is filter equivalent resistance. $v_s(k)$ is input voltage of IGBT bridge, which is in form of vector and calculated by

$$v_s(k)=\frac{2}{3}v_{dc}\cdot\begin{bmatrix}1 & \alpha & \alpha^2\end{bmatrix}\cdot S(k)\ . \tag{6}$$

Where $S(k)$ is optimal switch combination at time k, operator $\alpha=\exp(\mathrm{j}\cdot 2\pi/3)$.

And $i_s(k)$、$v_o(k)$、$i_o(k)$ showed in Fig.4 are all in form of vector and are calculated by operator α. $v_{op}(k+1)$ is prediction value of v_o at instant $k+1$.

Closed-loop correction is achieved by

$$\begin{cases} v_{cop\alpha}(k+1)=v_{op\alpha}(k+1)+\lambda_{c\alpha}\cdot[v_{cop\alpha}(k)-v_{o\alpha}(k)]\\ v_{cop\beta}(k+1)=v_{op\beta}(k+1)+\lambda_{c\beta}\cdot[v_{cop\beta}(k)-v_{o\beta}(k)]\end{cases}. \tag{7}$$

Where $v_{cop}=v_{cop\alpha}+\mathrm{j}v_{cop\beta}$ is correction value of v_{op}, and prediction value $v_{op}=v_{op\alpha}+\mathrm{j}v_{op\beta}$, measured value $v_o=v_{o\alpha}+\mathrm{j}v_{o\beta}$, $\lambda_{c\alpha}$ and $\lambda_{c\beta}$ are correction factors in real and imaginary axis respectively, there are $\lambda_{c\alpha}=\lambda_{c\beta}=\lambda_c$ and λ_c is calculated by (2).

Then $v_{opi}(k+2)$, i=0,…,7 are calculated by prediction model(5) and (3) with variables $v_{cop}(k+1)$ and λ_{c1}. The cost function of system is defined as

$$f_{gi}=(v_{o\alpha}^*-v_{opi\alpha})^2+(v_{o\beta}^*-v_{opi\beta})^2,\quad i=0,\dots,7\ . \tag{8}$$

Where $v_o^*=v_{o\alpha}^*+\mathrm{j}v_{o\beta}^*$ is reference of output voltage, and prediction value $v_{opi}=v_{opi\alpha}+\mathrm{j}v_{opi\beta}$.

The load-current observer designed in [16] is not included in FCS-MPCFC scheme, disturbance from load-current measure is treated as external interference and will be corrected.

IV. Simulation Analyses

In this section, 2L-VSI discussed in Section III part *B* is used to test FCS-MPCFC scheme. Simulation models of 2L-VSI and FCS-MPCFC scheme are developed by MATLAB/Simulink. Parameters of inverter circuit are v_{dc}=520V, L=2.4mH, C=40uF, r=0.05Ω, and control period is set to T_s=33us.The output voltage reference is symmetrical three-phase AC voltage with frequency f_{ref}=50HZ and amplitude A_{ref}=200V.

In order to analyze performance of FCS-MPCFC, circuit parameters in object simulation model are set different from prediction model (5), and model parameter mismatches in control process are created artificially. Then there are four types of model parameter mismatches, parameter match (M), resistance mismatch (RP, RS), capacitor mismatch (CS10, CP10, CS20, CP20), inductor mismatch (LS10, LP10, LS20, LP20). The symbols R, C, L mean resistance, capacitor and inductor. And S or P means parameters in object model are submitted or pulsed. The number 10 means capacitor or inductor parameters change 10% and 20 means 20%. In parameter match condition (M), parameters in object model and prediction model are accordant, but discretization modeling error in (5) is included.

In this paper, three types of load conditions are discussed, and they are no load condition, resistive-inductive load condition with active power P=15kW and reactive power Q=2kvar, nonlinear load condition constructed by diode bridge rectifier with paralleled load resistor 47Ω and load capacitor 470uF. In each load condition, THD value of A-phase output voltage and average value of minimum cost function (AMCF) are provided for different kinds of model parameter mismatches conditions. The simulation waveforms of A-phase output voltage in parameters match condition are provided as well.

The AMCF value is calculated by

$$\mathrm{AMCF}=\sum_{k=1}^{\infty}f_{g\min}(k)\Big/\sum_{k=1}^{\infty}k\ . \tag{9}$$

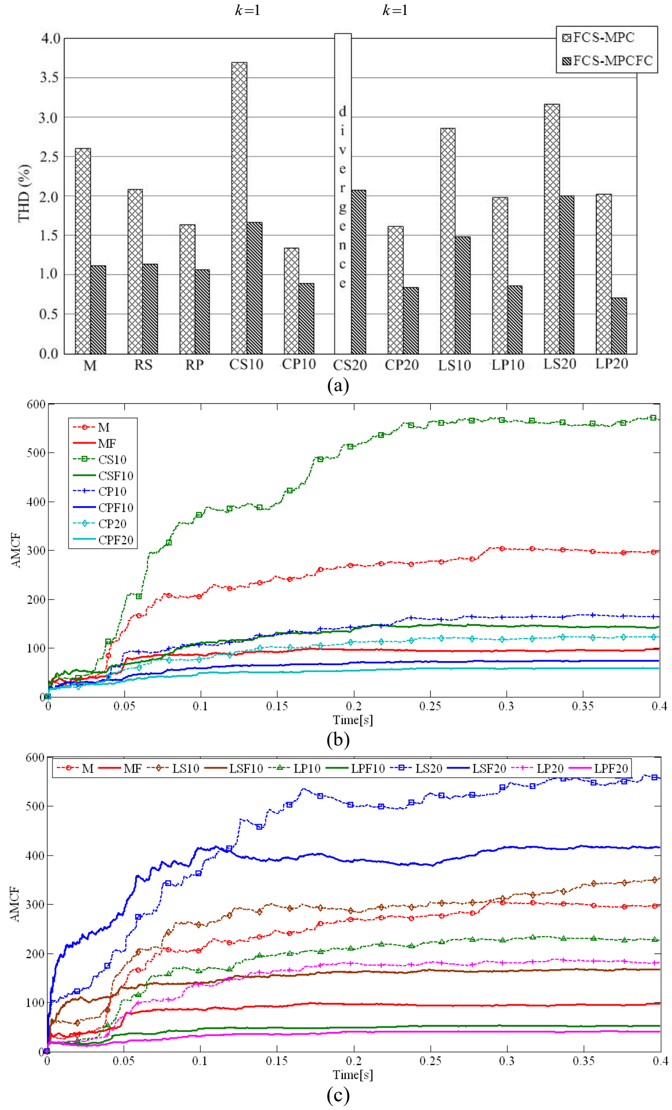

Fig. 5. Comparison analyses results in no load condition. (a) THD value.(b) AMCF curves of capacitor C mismatch. (c) AMCF curves of inductor L mismatch.

And $f_{gmin}(k)$ calculated by (8) is the minimum cost function at instant k, then AMCF means the average tracking error of output voltage.

A. No Load Condition

In no load condition, comparison analyses results and waveforms are showed in Figs.5-6. Fig.5(a) is THD value comparison histogram, and compared with FCS-MPC, FCS-MPCFC scheme significantly improves quality of output voltage for all types of parameter mismatches. Compared with parameter match condition M, under conditions of capacitor mismatches CS10, CS20 or inductor mismatches LS10, LS20, regardless of FCS-MPC and FCS-MPCFC scheme the quality of output voltage is reduced, especially in CS20 condition the control of FCS-MPC is divergence. But in conditions of CP10, CP20 or LP10, LP20, the control performance of both schemes are improved. So redundancy parameters design is beneficial for control scheme. In resistor parameter mismatch condition RS or RP, control performance of FCS-MPC scheme is improved, but FCS-MPCFC scheme is almost unaffected. The influences of parameter mismatches on FCS-MPCFC are smaller than which on FCS-MPC. It means that FCS-MPCFC is robust and adaptable.

In Fig.5(b) and (c), AMCF curves of FCS-MPC and FCS-MPCFC in no load condition are presented. The symbol F in legend means AMCF curves from FCS-MPCFC scheme and these curves are presented in bold lines. The corresponding dash lines with different markers are AMCF curves of FCS-MPC in the same parameter mismatch condition. For all kinds of mismatch conditions, average tracking errors of FCS-MPCFC are less than that of FCS-MPC and influences of different mismatch conditions on FCS-MPCFC scheme are smaller than that on FCS-MPC. In Fig.5(b) and (c), dash lines are scattered, but bold lines are close to each other, except LS20 condition.

Fig.6 shows the comparison simulation waveforms of A-phase voltage. Fig.6(a) and Fig.6(b) are A-phase voltage of inverter controlled by FCS-MPC and FCS-MPCFC respectively, and compared with Fig.6(a), in Fig.6(b) the quality of output waveform is improved.

B. Resistive-inductive Load Condition

The same analyses are proposed for resistive-inductive load condition in Figs.7-8. In Fig.7(a), THD values of inverter output voltage controlled by FCS-MPC and FCS-MPCFC scheme are presented, in all kinds of model parameter mismatches conditions, THD values of FCS-MPCFC are less than that of FCS-MPC. And compared with M, in resister parameter mismatch condition RS or RP, FCS-MPC decreases THD value, but THD values of FCS-MPCFC are almost kept stable. Then in CS10 and LS20 parameter mismatches conditions, regardless of FCS-MPC and FCS-MPCFC, the

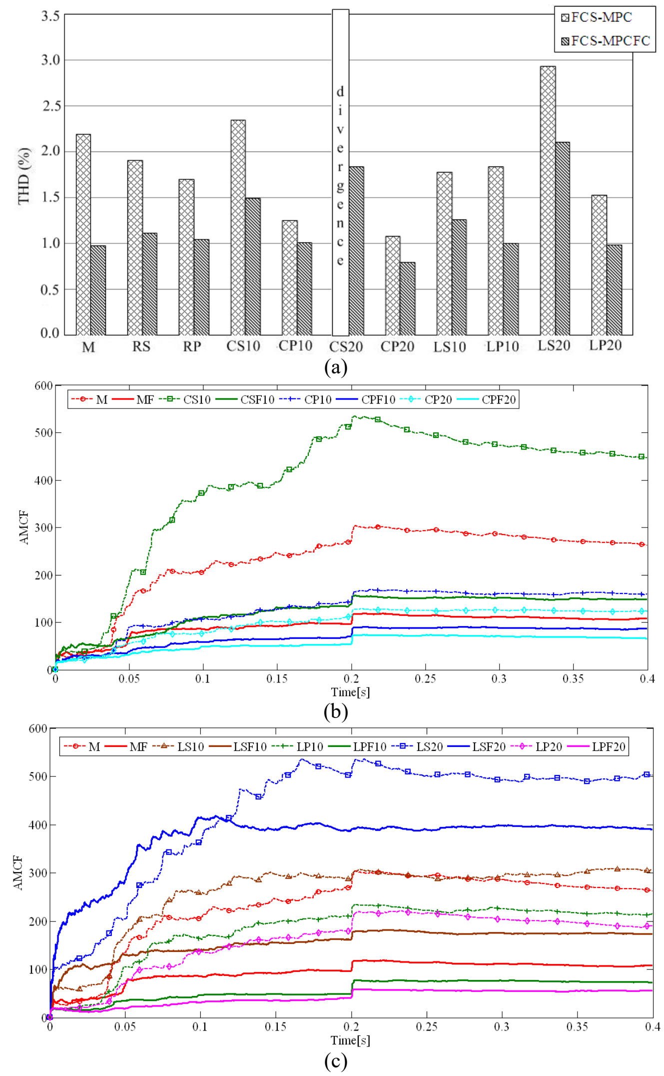

Fig. 7. Comparison analyses results in resistive-inductive load condition. (a) THD value.(b) AMCF curves of capacitor C mismatch. (c) AMCF curves of inductor L mismatch.

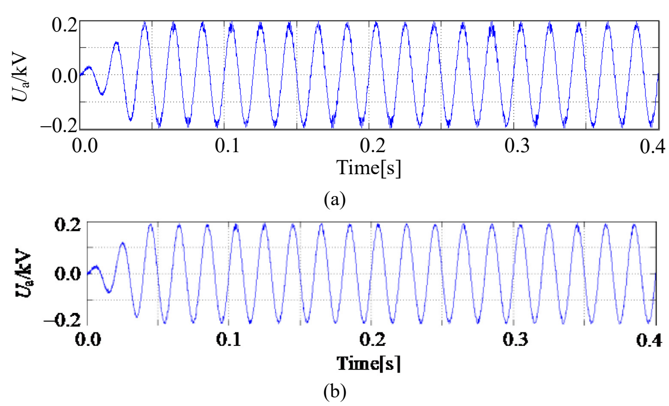

Fig. 6. Comparison simulation waveforms in no load condition. (a) FCS-MPC. (b) FCS-MPCFC

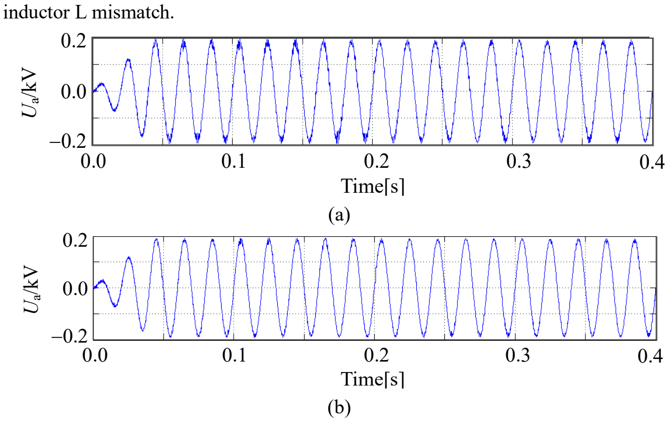

Fig. 8. Comparison simulation waveforms in resistive-inductive load condition. (a) FCS-MPC. (b) FCS-MPCFC

quality of output voltage become worse. But compared with FCS-MPC scheme, the influence of different parameter mismatches on FCS-MPCFC is smaller. Fig.7(b) and (c) are AMCF curves in resistive-inductive load condition, and load switch is closed at 0.2s. The minimum cost function value of FCS-MPCFC is less than that of FCS-MPC and parameter mismatch rejection ability of FCS-MPCFC is better than that of FCS-MPC, as curves belong to FCS-MPCFC are closer to each other.

Fig.8 shows the A-phase output voltage waveforms of inverter controlled by FCS-MPC and FCS-MPCFC respectively. After load switch is closed, the waveforms are improved both in Fig.8(a) and (b), but it is clearly indicated that the quality of waveform in Fig.8(b) is better than that in Fig.8(a).

C. Nonlinear Load Condition

In Figs.9-10, the control performances of FCS-MPC and FCS-MPCFC schemes on three-phase inverter in nonlinear load condition are presented. Fig.9(a) is THD value comparison histogram. Fig.9 (b) and (c) are AMCF curves in capacitor and inductor parameter mismatches conditions respectively. In Fig.9, it clearly shows that the THD and AMCF corresponding to FCS-MPCFC in all kinds of parameter mismatches conditions are less than that of FCS-MPC.Fig.10 shows the comparison simulation waveforms of A-phase output voltage. As in nonlinear load condition, the quality of waveforms are poor, but compared with FCS-MPC, FCS-MPCFC improves the quality of waveform.

D. Influence of Error Limen ε

In order to study influence of error limen ε in (2), the three-phase inverter with LS10 inductor parameter mismatch in no load condition is taken as an example. The AMCF curves of FCS-MPCFC scheme with different ε are presented in Fig.11. The legend c0, c10, c100 and c200 mean ε=0, 10, 100, 200 respectively. In Fig.11, the AMCF value declines with the increase of ε, but when ε=100, AMCF value is minimized, which means control performance is the best.

V. Experimental Results

FCS-MPCFC scheme for power converter is tested by a 2L-VSI prototype. The circuit parameters of this prototype and load are the same as that of simulation system in Section IV. The controller platform is constructed by DSP 28335. In the experiment system, there is no parameter mismatch in theory, but errors caused by components still exist. The experiment system is constructed by industrial level components, so feedback correction strategy in FCS-MPCFC works in practice. Comparison experiments are developed on traditional FCS-MPC and proposed FCS-MPCFC schemes. The A-phase voltage and current waveforms of 2L-VSI with resistive-inductive load and nonlinear load controlled by each scheme are showed in Figs.12-13.

In Fig.12, experimental results of FCS-MPC scheme are presented. Fig.12 (a) shows the A-phase voltage and current waveforms of 2L-VSI with resistive-inductive load, the THD of

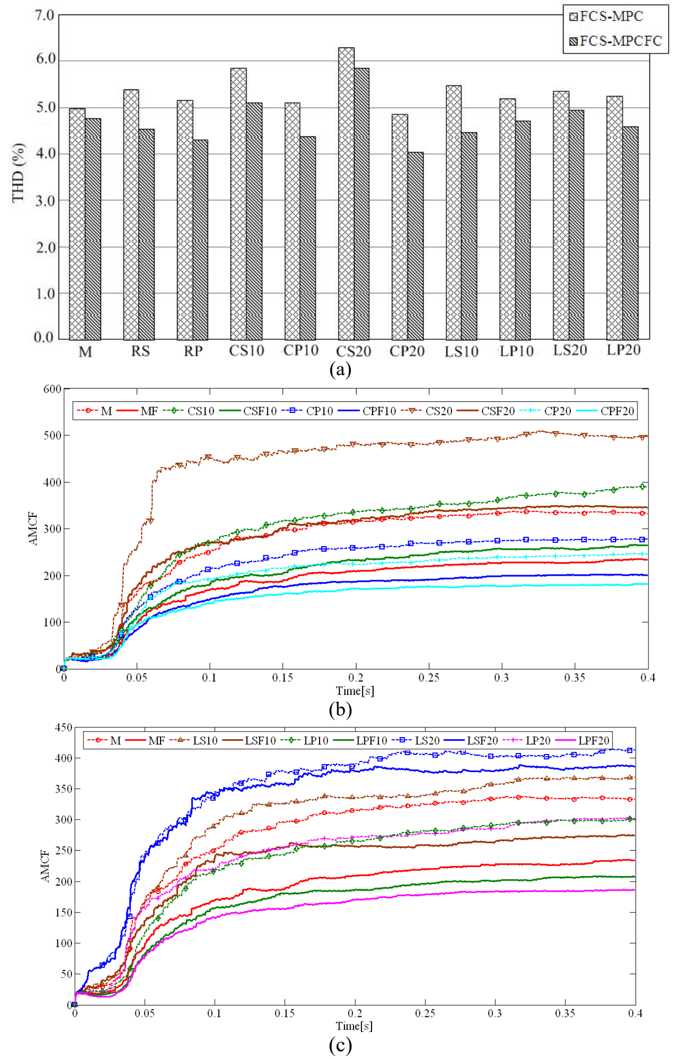

Fig. 9. Comparison analyses results in nonlinear load condition. (a) THD value.(b) AMCF curves of capacitor C mismatch. (c) AMCF curves of inductor L mismatch.

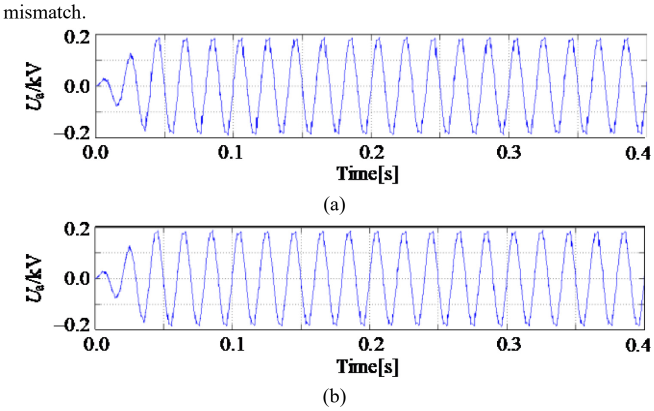

Fig. 10. Comparison simulation waveforms in nonlinear load condition. (a) FCS-MPC. (b) FCS-MPCFC

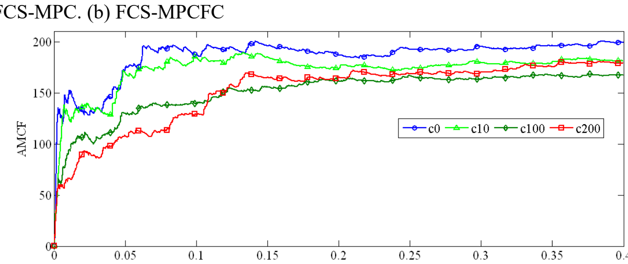

Fig. 11. Influence of error limen ε.

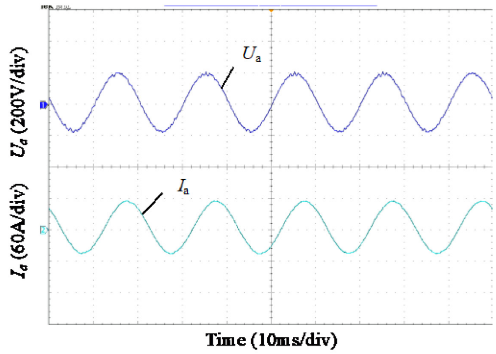

(a)

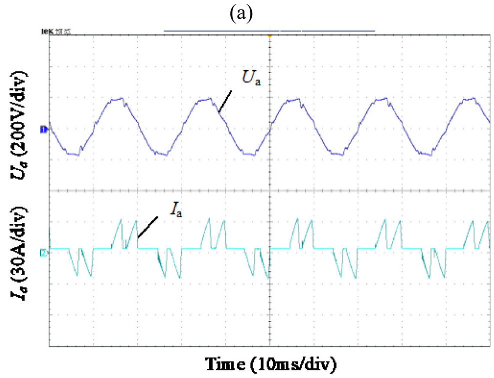

(b)

Fig. 12. Experimental results of FCS-MPC. (a) Resistive-inductive load. (b) Nonlinear load.

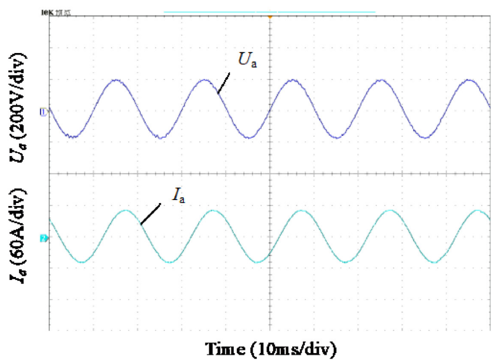

(a)

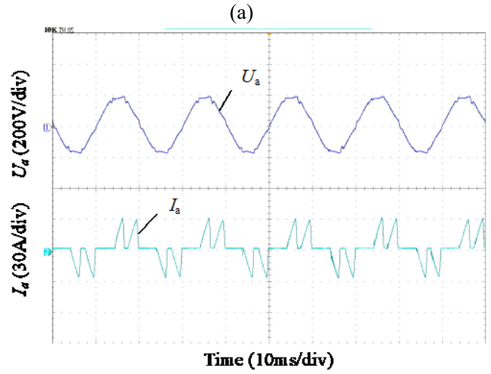

(b)

Fig. 13. Experimental results of FCS-MPCFC. (a) Resistive-inductive load. (b) Nonlinear load.

voltage waveform is 2.3%. The experimental waveforms of 2L-VSI with nonlinear load are shown in Fig.12 (b), and the THD of A-phase voltage waveform is 5.2%. The same experimental waveforms of 2L-VSI controlled by FCS-MPCFC scheme are presented in Fig.13 for comparison purpose. Fig.13(a) shows the experimental waveforms of 2L-VSI with resistive-inductive load, and the THD of voltage is 1.1%. The experimental waveforms of 2L-VSI with nonlinear load are showed in Fig.13(b), and the THD of voltage waveform is 4.9%.

It is clearly indicated that, compared with FCS-MPC scheme, FCS-MPCFC scheme improves the control performance of 2L-VSI in the same load condition.

VI. Conclusion

In traditional FCS-MPC algorithm, the influence of model parameter mismatches and environment disturbance is ignored, and the control performance is impacted. Then a feedback correction strategy for FCS-MPC scheme is proposed, which is achieved by adjusting output of prediction model with actual value. The simulation and experimental results indicate that the proposed strategy enhances the robustness and adaptation of FCS-MPC scheme. Although the proposed FCS-MPCFC scheme compensates output of prediction model, the prediction model itself is not adjusted. A more accurate correction algorithm will be studied in the next work.

References

[1] Xi Yugeng, *Predictive Control*, 2nd ed. Beijing, China: National Defense Industry Press, 2013.

[2] J. Rodriguez, M.P. Kazmierkowski, J.R. Espinoza, P Zanchetta, H. Abu-Rub, H.A. Young and C.A. Rojas, “State of the art of finite control set model predictive control in power electronics,” *IEEE Trans. Ind. Informat.*, vol.9, no.2, pp.1003–1016, May 2013.

[3] J. Rodriguez, P. Cortes. *Predictive control of power converters and electrical drives*, 1st ed. Chichester, U.K.: IEEE Wiley Press, 2012.

[4] P. Cortes, J. Rodriguez, C. Silva and A. Flores, “Delay compensation in model predictive current control of a three-phase inverter,” *IEEE Trans. Ind. Electron.*, vol.59, no.2, pp. 1323–1325, Feb.2012.

[5] R. P. Aguilera, P. Lezana and D. E. Quevedo, “Finite-control-set model predictive control with improved steady-state performance,” *IEEE Trans. Ind. Informat.*, vol.9, no.2, pp. 658–667, May. 2013.

[6] M. Preindl, E. Schaltz and P. Thogersen, “Switching frequency reduction using model predictive direct current control for high-power voltage source inverters,” *IEEE Trans. Ind. Electron.*, vol.58, no.7, pp. 2826–2835, Jul.2011.

[7] C.A. Rojas, J. Rodriguez, F. Villarroel, J.R. Espinoza, C.A. Silva and M. Trincado, “Predictive torque and flux control without weighting factors,” *IEEE Trans. Ind. Electron.*, vol.60, no.2, pp. 681–690, Feb.2013.

[8] C. D. Townsend, R. A. Baraciarte, Y. Yu, D. Tormo, H. Zelaya de La Parra, G. D. Demetriades and V. G. Agelidis, “Heuristic Model Predictive Modulation for High-Power Cascaded Multilevel Converters,” *IEEE Trans. Ind. Electron.*, vol. 63, no. 8, pp. 5263–5275, Aug. 2016.

[9] T. Geyer and D. E. Quevedo, “Performance of multistep finite control set model predictive control for power electronics,” *IEEE Trans. Power Electron.*, vol.30, no.3, pp. 1633–1644, Mar. 2015.

[10] Kun Shen and Jing Zhang, “Modeling error compensation in FCS-MPC of a three-phase inverter,” in *Proc. IEEE Int. Conf. Power electron., Drives Energy Syst.*, Bengaluru, India, 2012, pp.1–6.

[11] Young H A, Perez M A and J. Rodriguez, “Analysis of finite control set model predictive current control with model parameter mismatch in a three phase inverter,” *IEEE Trans. Ind. Electron.*, vol. 63, no.5, pp. 3100–3107, May.2016.

[12] Junxiao Wang, Fengxiang Wang, Zhenbin Zhang, Shihua Li and J. Rodriguez, “Design and Implementation of Disturbance Compensation-Based Enhanced Robust Finite Control Set Predictive Torque Control for Induction Motor Systems,” *IEEE Trans. Ind. Informat.*, vol. 13, no. 5, pp. 2645–2656, Oct. 2017.

[13] C. Dirscherl and C. M. Hackl, “Model predictive current control with analytical solution and integral error feedback of doubly-fed induction generators with LC filter,” in *Proc. IEEE International symposium on*

predictive control of electrical drives and power electronics,Brasov, Romania,2017, pp. 25–30.

[14] Rodrigo Mendez, Daniel Sbarbaro, Jose Espinoza and Christian Rojas, “Finite Control Set Model Predictive Control Assisted by a Linear Controller for True Parameter Uncertainty Compensation,” in *Proc. IEEE Energy conversion congress and exposition*, Cincinnati, USA, 2017, pp. 4964–4970.

[15] Morcos Metry and Robert S. Balog, “A parameter mismatch study on model predictive control based on sensorless current mode,” in *Proc. IEEE Texas power and energy conference*, Texas, USA, 2018, pp.1–6.

[16] P. Cortes, G. Ortiz, J. I. Yuz, J. Rodriguez, S.Vazquez and L.G. Franquelo, “Model predictive control of an inverter with output LC filter for UPS applications,” *IEEE Trans. Ind. Electron.*, vol. 56, no. 6, pp. 1875–1883, Jun.2009.

Kun Shen received the B.S. degree from North China University of Science and Technology, Tangshan, China, in 2006, and the Ph.D degree from Hunan University, Changsha, China, in 2012.

He is currently a postdoctoral researcher with the College of Electrical and Information Engineering, Hunan University, Changsha, China. Since 2012, he has been with the College of Information Science and Engineering, Hunan Normal University, Changsha, China, where he became an Assistant Professor in 2013. His research interests include power electronics, model predictive control and wind energy generation.

Jianghua Feng was born in Hengyang, Hunan, China, in 1964. He received the B.S. and M.S. degrees in Electrical engineering from the Zhejiang University, Zhejiang, China, in 1989, and the Ph.D. degree in control engineering from Central South University, Changsha, China, in 2008.

Since 1989, He has been with the Zhuzhou CRRC Times Electric Co., Ltd., Zhuzhou, where from 2002 to 2004, he was the Director of Technology Center, and from 2005 to 2009, he was the Technical Director of Zhuzhou CRRC Times Electric Co., Ltd., and, currently is the Chief Engineer. His research interests are in power electronics, drive control, and permanent magnet motor system.

Prof. Feng was a recipient of the Mao Yisheng prize for science and technology of China, and the honorary title of Contemporary Inventor of China in 2016.

Jing Zhang received the B.S., M.S., and Ph.D. degrees in control engineering from Hunan University, Changsha, China, in 1982, 1984, and 1997, respectively.

Since 1984, He has been with the college of electrical and information engineering, Hunan University, where from 1998 to 2001, he was the Director and, currently, is a Professor. From 2002 to 2013, he was the Vice-Rector of the Hunan University. His research interests are in optimal control, model predictive control, and intelligent control for complex industry system.

Prof. Zhang was a recipient of China national second prize of scientific and technological progress. And since 2000, he expert with state department special allowance of china, he also is the CSM senior member.